Colloid Polym Sci (2009) 287:715–723
DOI 10.1007/s00396-009-2011-6

ORIGINAL CONTRIBUTION

Influence of clay modification on the properties of aramid-layered silicate nanocomposites

**Sonia Zulfiqar · Muhammad Rafique ·
Muhammad Sajjad Shaukat · Muhammad Ishaq ·
Muhammad Ilyas Sarwar**

Received: 3 December 2007 / Revised: 20 December 2008 / Accepted: 28 January 2009 / Published online: 26 February 2009

Abstract Nanocomposites from organoclay and aromatic polyamide were prepared using solution intercalation method. Aramid chains were synthesised by reacting 4-aminophenylsulfone with isophthaloyl chloride in dimethylacetamide. Dodecylamine was used as a modifier to change the hydrophilic nature of montmorillonite into organophilic. Suitable quantities of organoclay were mixed in the aramid solution with high-speed stirring for homogeneous dispersion of the clay. Thin films cast from these materials after evaporating the solvent were characterised. The morphology of nanocomposites was determined by X-ray diffraction and TEM. Results revealed the formation of delaminated and disordered intercalated clay platelets in the aramid matrix. Mechanical data indicated improvement in the tensile strength and modulus with clay loading up to 6 wt.%. The glass transition temperature increased up to 20 wt.% organoclay, suggesting better cohesion between the two phases and thermal stability augmented with increasing clay loading. The water uptake reduced gradually as a function of organoclay showing decreased permeability.

Keywords Aramid · Organoclay · Nanocomposites · Thin films · XRD · TEM · Mechanical properties · TGA · DSC · Water uptake

S. Zulfiqar · M. Rafique · M. S. Shaukat · M. Ishaq ·
M. I. Sarwar (✉)
Department of Chemistry, Quaid-i-Azam University,
Islamabad 45320, Pakistan
e-mail: ilyassarwar@hotmail.com

M. I. Sarwar
Department of Materials Science and Engineering,
University of Delaware,
Newark, DE 19716, USA

Introduction

Polymer clay nanocomposites are a new class of materials that have gained considerable interest in recent years owing to their enhanced stiffness, strength and barrier properties at very low loading levels of organophilic clay as compared to the conventional filler composites [1–12]. These composites form a novel fundamental scientific subject on account of nanoscale incorporation of filler into the polymer matrix. The incompatibility between organophilic polymer and the hydrophilic layered silicates has been resolved through surface modification of the clays. This is accomplished via an ion exchange reaction of the surface sodium ions with organics producing organically modified layered silicates. The replacement of inorganic exchange cations by organic onium ions on surface of clay not only serves to match the clay surface polarity with the polarity of the polymer but also expands the interlayers of clay, thus facilitating the penetration of polymer precursors or preformed polymer. Depending on the charge density of clay and the onium ion surfactant, different arrangements of the onium ions are possible. However, long chain surfactant and high charge density of the clay forced the clay nanolayers further apart. Depending on the charge density of clay, the onium ion may lie parallel to the clay surface as monolayer, a lateral bilayer, a pseudo-trimolecular or an inclined paraffin structure. At very high charge densities, large surfactant ions can adopt lipid bilayer orientations in the clay interlayers. The orientations of onium ion chains in organoclay were initially deduced based on infrared and X-ray diffraction (XRD) measurements [13–15]. More modelling experiments have provided further insights into the packing orientation of the alkyl chains in organically modified layered silicates [16].

Within the field of polyamide based clay nanocomposites, several studies have focussed on aliphatic polyamides [17–22] but no attention has been paid so far to the aromatic polyamides. Aromatic polyamides commonly known as aramids have been noted for their excellent characteristics such as high thermal stability, good chemical resistance and excellent mechanical properties. These polymers present solubility problems as matrices for organoclay nanocomposites. Most polyamides are intractable because of their low solubilities in the organic solvents. By making these polymers more tractable, soluble and processable without sacrificing their properties can make them a good candidate for further advanced applications [23–26]. One of the most common approaches to increasing solubility, lowering glass transition (T_g) and softening temperatures (T_s) is the incorporation of flexible or bulky substituents as pendent groups, and using an optimal minimum amount of meta linkages (producing a few kinks) along the backbone of such polymers generally increases the solubility and/or thermo-plasticity of aramids [27–31]. These groups impart an enhanced solubility, processability and toughness of the polymers without substantial attenuation of thermal properties. Various types of hybrid materials based on polyamides have been documented by the present authors [32–39].

The aim of this study is to focus on some new nanocomposite materials prepared by introducing organoclay into the aramid matrix. The polymer chains employed were prepared by reacting 4-aminophenylsulfone with isophthaloyl chloride in dimethyl acetamide as a solvent. Compatibility between the polymer and hydrophilic montmorillonite was achieved by intercalation of the clay with dodecylamine. The aramid chains were then blended with different proportions of organoclay, and the nanocomposites thus obtained were characterised with regards to their XRD, TEM, mechanical properties, thermogravimetric analysis (TGA), differential scanning calorimetry (DSC) and water uptake.

Experimental section

Materials

Isophthaloyl chloride (IPC), triethylamine (TEA) and hydrochloric acid obtained from Fluka were used as such. *N*,*N*-Dimethyl acetamide (DMAc) was procured from Aldrich and dried over molecular sieves before use. 4-Aminophenylsulfone (APS), montmorillonite K-10 (cation exchange capacity 119 meq/100 g), dodecylamine (DDA) and silver nitrate were obtained from Aldrich and used as received. The chemical composition of montmorillonite K-10 is reported to be SiO_2 (43.77%), Al_2O_3 (18.57%), CaO (1.02%), Na_2O (1.13%) and H_2O (36.09%) [40].

Preparation of DDA-MMT

Ion exchange method was used to prepare organically modified MMT. Dodecylamine was placed in a beaker, followed by the addition of concentrated hydrochloric acid and water. This solution was heated at 80°C. In another beaker, montmorillonite was dispersed in water at 80°C. Both the solutions were mixed, and the resulting mixture was agitated vigorously for 3 h at 60°C. The precipitates of organoclay were isolated, washed by placing in hot water with constant stirring for 1 h and then filtered. This process was repeated to remove the residual ammonium salt of dodecylamine. The filtrate was titrated with 0.1 N $AgNO_3$ until there was no AgCl precipitates to ensure a complete removal of chloride ions. The final product obtained by filtration was dried in a vacuum oven at 60°C for 24 h. The dried cake was ground and screened with a 325-mesh sieve. This modified clay was designated as DDA-MMT and was used for the preparation of nanocomposites.

Synthesis of aramid matrix

Aramid chains were generated by condensing aromatic diamine with aromatic diacid chloride at low-temperature under inert conditions. The reaction was carried out in a 250 ml flask provided with a stirrer by placing 0.05 mol of 4-aminophenylsulfone, followed by the addition of DMAc as a solvent. After complete mixing, the amine solution was cooled to 0°C, and then IPC (0.05 mol) was added under anhydrous conditions with constant stirring at low temperature for 1 h. The temperature of flask was then raised to 25 °C. The reaction between diamines and diacid chloride is

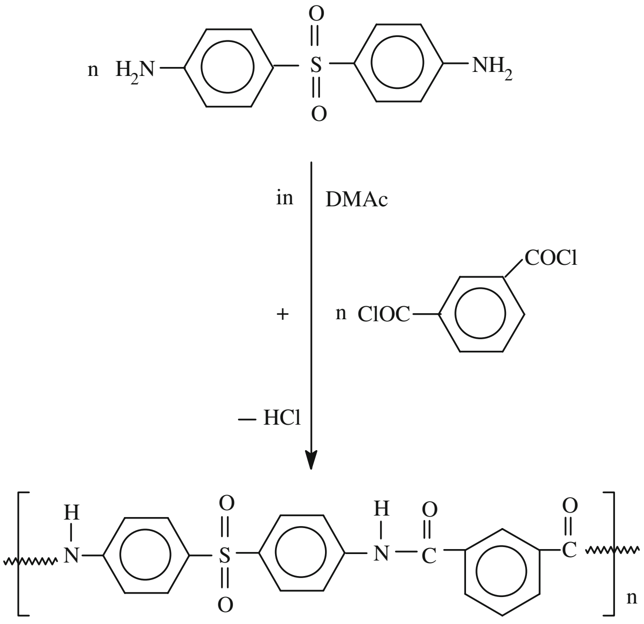

Scheme 1 Formation of aramid chains

extremely fast; even then, the reaction mixture was agitated overnight to ensure the completion of reaction. The reaction mixture is highly viscous and golden in colour. The chemical reaction leading to the formation of aromatic polyamide chains is given in Scheme 1. The HCl produced from the aramid solution was removed by adding stoichiometric amount of TEA with constant stirring of 3 h. The precipitates were separated by centrifugation method and the neat aramid was decanted. The polymer resin thus prepared served as a stock solution for the fabrication of nanocomposites.

Synthesis of aramid/DDA-MMT nanocomposites

In order to prepare nanocomposites, various proportions of DDA-MMT (2 to 20 wt.%) were added to the aramid solution with high speed stirring for 24 h at 25 °C. Hybrid films were obtained by pouring the composite solutions into petri dishes placed on a levelled surface. The solvent was evaporated at 70 °C for 12 h. These films were further dried at 80 °C under vacuum to a constant weight. The flow sheet and schematic representation for the formation of nanocomposites are given in Schemes 2 and 3.

Characterisation

The diffraction pattern of aramid based nanocomposites was studied in the reflection mode using a Philips PW 1820 diffractometer. Nickel-filtered Cu Kα radiation (radiation wavelength, $\lambda = 0.154$ nm) was produced by a PW 1729 X-ray generator at an operating voltage of 40 kV and a current of 30 mA. The scanning angle for all measurements was kept between $2\theta = 2°$ and $10°$ with a step size of 0.02° to measure the change in interlayer spacing of clay based on

Scheme 2 Flow sheet diagram for the synthesis of aramid/DDA-MMT nanocomposites

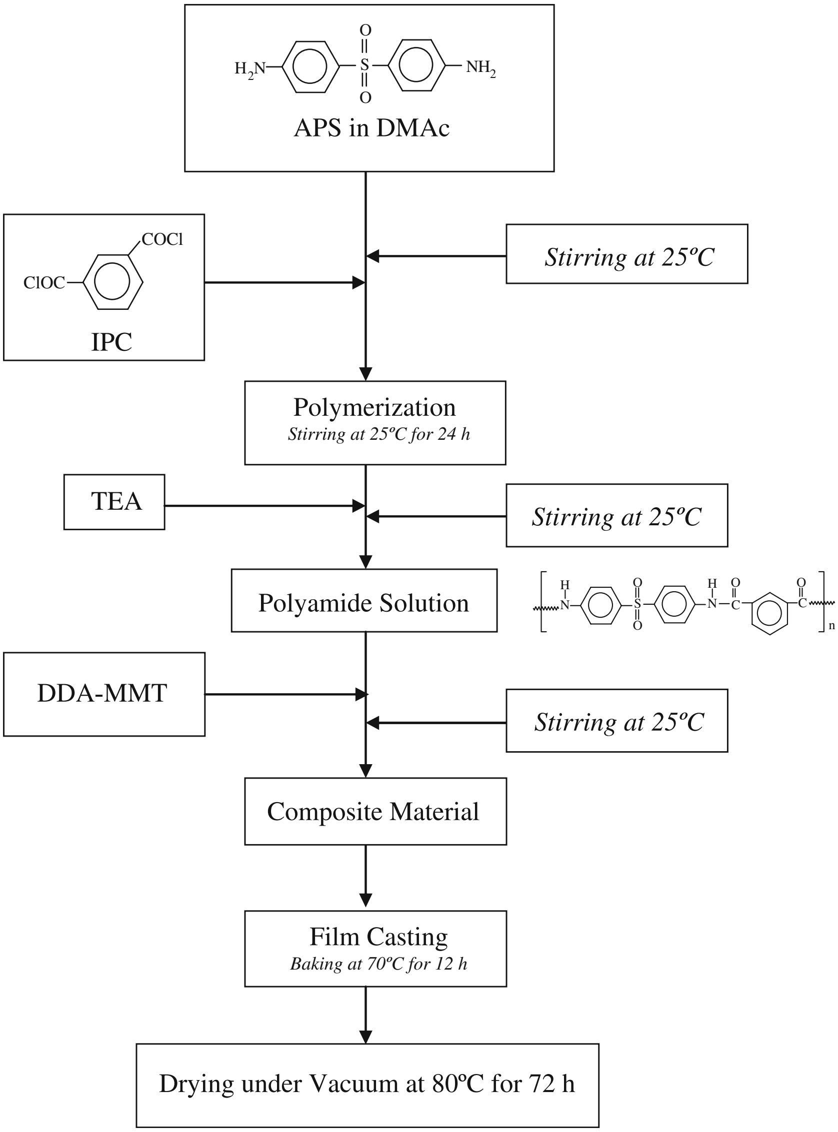

Bragg's law. The wetting and disaggregation properties of surface modified montmorillonites have already been well documented in literature [13–16]. The microstructure of nanocomposites was imaged by using FEI Tecnai F20 transmission electron microscope operated at an accelerating voltage of 200 kV. The hybrid films were first microtomed into 60 nm ultra-thin sections with a diamond knife using Leica Ultracut UCT ultramicrotome. Tensile properties of thin hybrid films were measured according to DIN procedure 53455 at 25 °C using Testometric Universal Testing Machine M350/500, and an average value obtained from five to seven different measurements in each case has been reported. The thermal stability of nanocomposites was determined using a METTLER TOLEDO TGA/SDTA 851^e

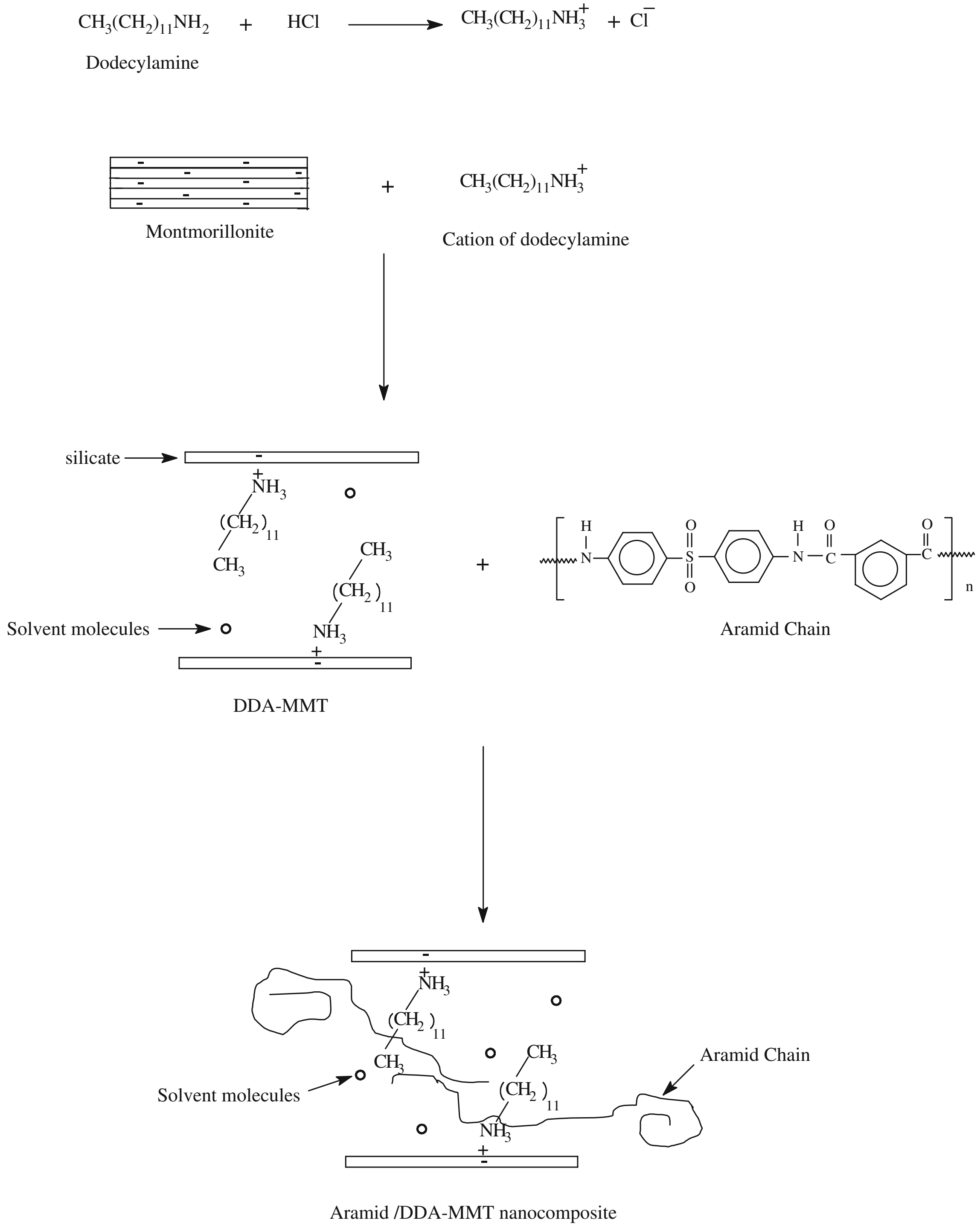

Scheme 3 Schematic representation for the formation of aramid/DDA-MMT nanocomposites

thermogravimetric analyzer using 1–5 mg of the sample in Al_2O_3 crucible heated from 25 to 600 °C at a heating rate of 10 °C min^{-1} under nitrogen atmosphere with a gas flow rate of 30 ml min^{-1}. Thermomechanical properties of the nanocomposites were characterised using a METTLER TOLEDO DSC 822^e differential scanning calorimeter. For determining the glass transition temperatures, samples of 5 −10 mg were encapsulated in aluminium pans and heated at a ramp rate of 10 °C/min under nitrogen atmosphere.

The water uptake of aramid/DDA-MMT nanocomposites were carried out under the specifications of ASTM D570-81. The films were placed in a vacuum oven at 80 °C till the films attained a constant weight and then weighed out to get the initial weight (W_o). The films were immersed in deionised water at 25 °C. After 24 h, the films were removed from water, and then they were quickly placed between sheets of filter paper to remove the excess water, and films were weighed immediately. The films were again soaked in water. After another 24-h soaking period, the films were removed, dried and weighed for any weight gain. This process was repeated till the films almost attained the constant weight. The total soaking time was 168 h, and the samples were weighed at regular 24-h time intervals to get the final weight (W_f). The percent increase in weight of the samples was calculated by using the formula $(W_f - W_o)/W_o$.

Results and discussion

The chemical structure, molecular weight and solution properties of the aramid matrix have already been documented in our recent reports [41, 42]. Thin film obtained from the neat aramid was transparent and golden in colour. This colour was changed to light brown upon the addition of organoclay. The transparency of composite films decreased gradually by the addition of clay, and the films became semitransparent as well as brittle at high loading of organoclay. Results obtained from the characterisation of these materials using various techniques are reported.

X-ray diffraction

The XRD patterns of MMT, DDA-MMT and nanocomposites containing various proportions of organoclay mixed with aramid are presented in Fig. 1. The primary silicate reflections at 2θ = 8.78° for MMT and at 2θ = 5.82° for DDA-MMT corresponded to d-spacing of 1.006 and

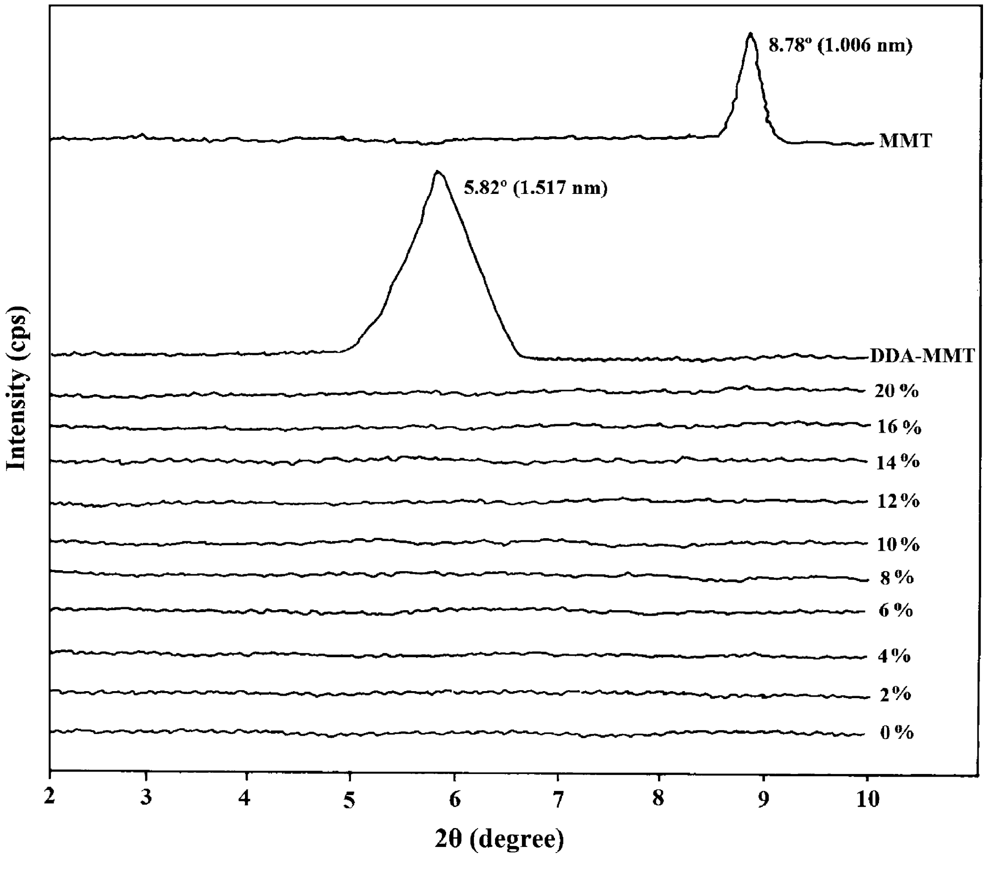

Fig. 1 X-ray diffraction pattern of aramid/DDA-MMT nanocomposites

Fig. 2 TEM micrographs of aramid/DDA-MMT nanocomposites **a** 4, **b** 10, **c** 20 wt.% ▶

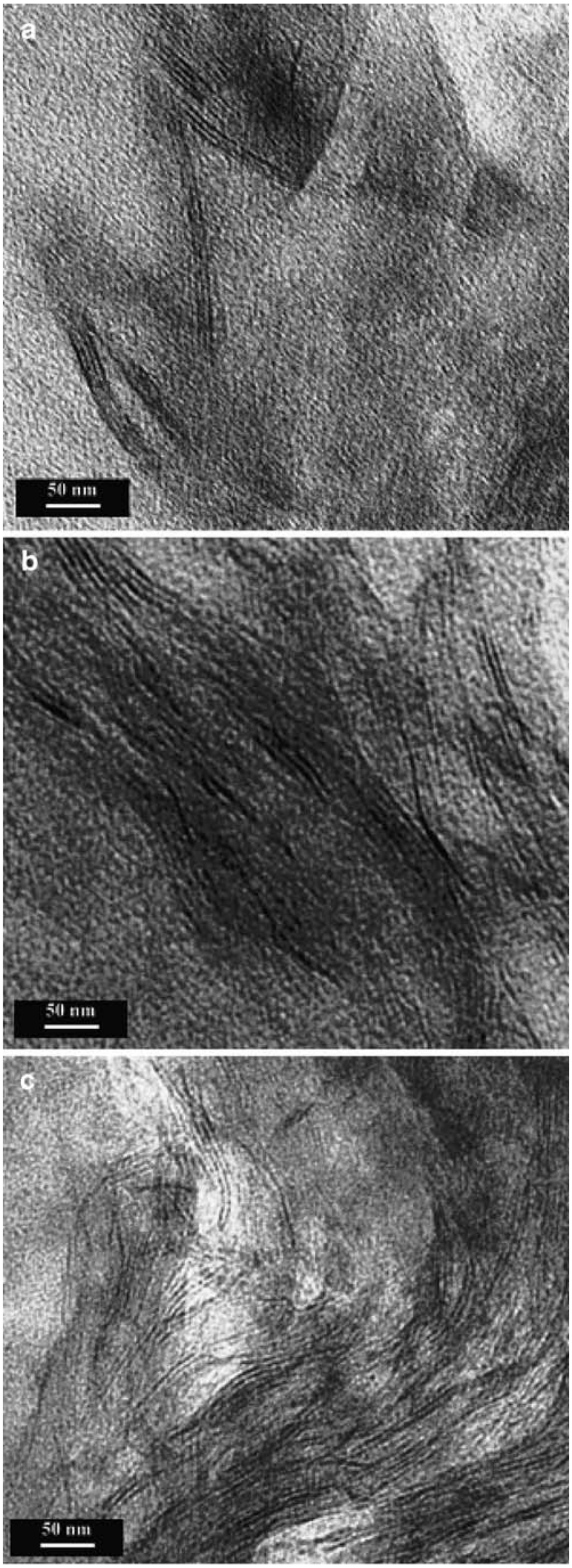

1.517 nm respectively, confirming that MMT becomes organophilic. Furthermore, the intensity of peak becomes stronger, implying that the layers of clay become much more ordered. After mixing of organoclay with aramid resin, the diffraction peak disappeared, indicating disruption of clay layers in the matrix. Organoclay nanocomposites having 2 to 20 wt.% DDA-MMT content gave no characteristic diffraction peak in small-angle region, indicating the formation of delaminated hybrid materials. The development of nanostructures depends on the nature of alkyl ammonium exchanged clays. Longer linear alkyl chains generally facilitate the formation of nanocomposites.

Transmission electron microscopy

The morphology of aramid/DDA-MMT nanocomposites was studied using TEM, and the images of hybrid films containing 4, 10 and 20 wt.% organoclay are given in Fig. 2a, b and c, respectively. Both disordered delaminated and disordered intercalated morphologies were observed for these nanocomposites. The micrograph of polyamide with 4 wt.% organoclay loading gave well-dispersed nanolayers with an interlayer spacing of 10–20 nm (Fig. 2a), which are larger than the original spaces between silicate layers in the organoclay, suggesting the formation of delaminated nanocomposites. On further addition of organoclay (10 and 20 wt.%) in the nanocomposites, partially exfoliated and disordered intercalated nanostructures are obtained as seen from Fig. 2b and c. These morphologies clearly show individual silicate platelets dispersed in the host matrix as well as some stacking of silicate layers, but the dimensions of these conglomerations are too small to present any diffraction peak in the XRD pattern. The overall morphology of the system is disordered delaminated and disordered intercalated at higher loading of clay contents. TEM observations of these materials suggested a good dispersion of organoclay in the polyamide matrix at low concentration. However, samples having higher amounts of organoclay exhibited mixed morphologies with stacking of the clay layers.

Mechanical properties

The stress–strain data for linear aramid/DDA-MMT composite films are given in Table 1 (Fig. 3). Tensile strength of the hybrid materials increased relative to the pure aramid with increasing organoclay. The tensile modulus calculated from the stress–strain isotherms for neat aramid had a value of 578.8 MPa that increased to a maximum value

Table 1 Mechanical, glass transition temperatures and water absorption data of aramid/DDA-MMT nanocomposite materials

DDA-MMT contents (%)	Maximum stress (MPa)±0.10	Maximum strain±0.02	Initial modulus (MPa)±0.02	Toughness (MPa)±0.20	T_g (°C)	Water absorption at equilibrium (%)
0.0	35.61	0.131	578.81	3.759	78.00	9.4
2.0	47.14	0.114	884.82	4.085	–	8.3
4.0	50.78	0.091	901.76	3.222	78.64	7.8
6.0	51.85	0.073	1012.7	2.635	–	6.7
8.0	50.19	0.067	831.68	2.087	87.17	5.8
10.0	46.35	0.059	800.92	1.685	–	4.9
12.0	45.56	0.053	778.95	1.395	92.32	4.5
14.0	43.78	0.051	724.33	1.214	–	3.6
16.0	37.74	0.049	711.44	1.014	106.95	2.5
20.0	36.66	0.043	629.77	0.779	119.00	0.4

1,012.7 MPa with 6 wt.% of DDA-MMT, beyond this, it decreased. The modulus of a polymeric material improved when nanocomposites are formed with nanolayers. The improvement in tensile modulus of aramid nanocomposites is due to the strong hydrogen bonding between the two phases and average length of the dispersed clay platelets (aspect ratio). The disordered delaminated silicate layers with high aspect ratio in aramid with 4 to 6 wt.% loading of DDA-MMT provide uniform dispersion as observed by TEM (Fig. 2a), resulting in modulus enhancement. The maximum increase in the stress was observed with 6 wt.% organoclay up to 51.85 MPa in the nanocomposites relative to the neat polyamide (35.6 MPa) and then gradually decreases with further loading of organclay. These results prove enhancement in the tensile strength of nanocomposites as compared to the neat polyamide. The stress is much more efficiently transferred from the polymer matrix to the inorganic filler resulting in enhanced tensile properties. Optimum tensile strength for nanocomposites is achieved when the concentration of clay is small, particularly up to 6 wt.% DDA-MMT in aramid matrix. At high clay loading, silicate layers may stack together, and intergallery space do not increase much, disallowing further diffusion of the polyamide chains, thus reducing the mechanical properties. The elongation at break of nanocomposites decreased relative to pristine aramid, and toughness almost gave similar behaviour (Table 1). This trend may be explained on the basis of stacking of clay platelets, possibly, forming conglomerates. This may lead the distribution of the silicate layers in the matrix non-homogeneous, thus increasing the numbers of defects or flaws in the composite materials causing brittleness and deterioration in the mechanical properties.

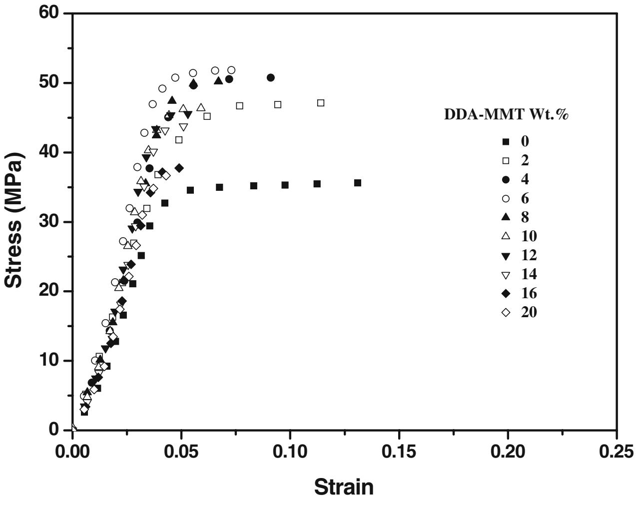

Fig. 3 Stress–strain curves of aramid/DDA-MMT nanocomposites

Thermogravimetric analysis

The thermal behaviour of aramid/DDA-MMT nanocomposites is shown in Fig. 4. Thermograms indicate that decomposition temperatures of these materials are in the range 225–450 °C, which means that these nanocomposites are thermally stable that slightly increases with addition of clay content in the aramid matrix. Incorporation of clay into the polymer matrix was found to enhance thermal stability by acting as a superior insulator and mass transport barrier to the volatile products generated during decomposition. The weight retained by these samples at 600 °C is roughly proportional to the amount of organoclay in the nanocomposites.

Differential scanning calorimetry

The glass transition temperature causes a shift in baseline of DSC scan when polymer changes from rigid to flexible form, and the related glass transition data are presented in Table 1 and Fig. 5. The results revealed maximum increase in the T_g value with 20 wt.% addition of organoclay. Glass

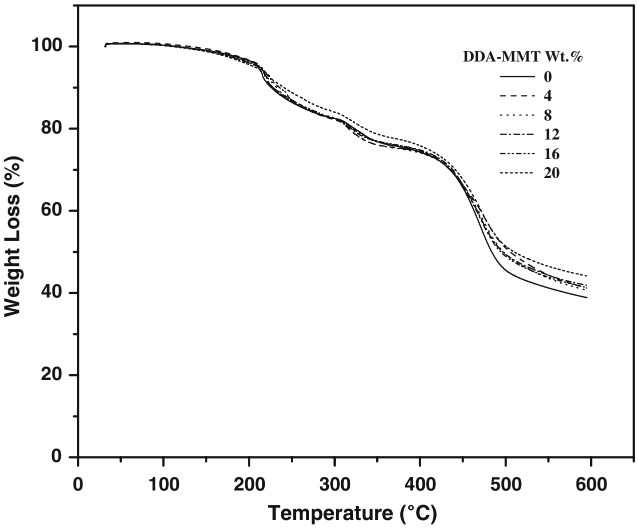

Fig. 4 TGA curves for aramid/DDA-MMT nanocomposites obtained at a heating rate of 10°C min^{-1} in nitrogen

transition temperatures of nanocomposites increased as compared to neat aramid in all the composite samples studied. This behaviour may be explained due to the intercalation of polymer chains into the interlayers of clay, suppressing mobility of the polymer segments near the interface. The change of glass transition temperature of the nanocomposites relative to pure polymer is attributed to the interaction between the filler and matrix at interfacial zones. The shift in baseline of DSC plot is due to restricted motion of the polymer chains resulting in high T_g values, particularly up to 119°C with 20 wt.% addition of DDA-MMT in this system. Aramid-based DDA-MMT nanocomposites showed a systematic increase in the T_g values upon the addition of nanoclay.

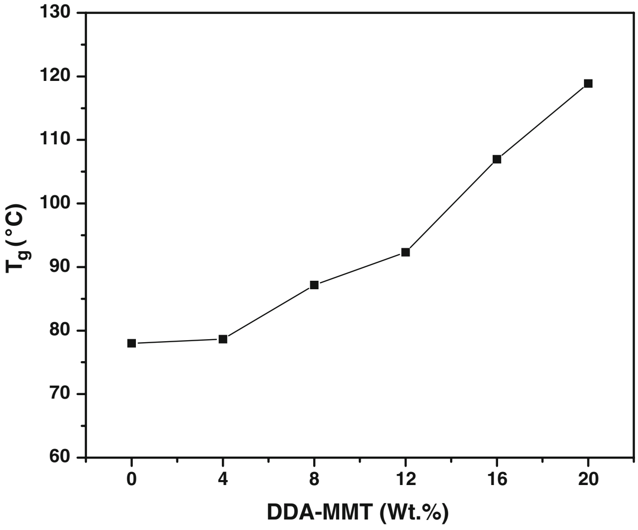

Fig. 5 Variation of glass transition temperatures as a function of DDA-MMT content in the nanocomposites

Water uptake measurements

The composite samples containing 2 to 20 wt.% clay were analysed for water uptake, and the corresponding data of each sample measured at saturation point are indicated in Fig. 6. This study is necessary as the aramid contain polar amide groups, which have a tendency to uptake water, subsequently deteriorating the mechanical properties of polyamide. It was observed that the water uptake for neat aramid film was optimum after 168 h (9.4%) that gradually decreases with increasing clay content. It is apparently due to the mutual physical interaction between the organic and inorganic phases, resulting in lesser availability of amide groups to interact with water. So, the presence of clay layers reduces the secondary bond forces between water molecules and the polar amide groups.

Conclusions

Incorporation of DDA-MMT reinforces the aramid matrix, representing compatibility between the two disparate phases. The interaction between organic and inorganic phases can be attained when nanolayers are completely dispersed throughout the matrix. This is possible when the amount of organoclay is small particularly up to 6 wt.% in aramid/DDA-MMT nanocomposites. At low loading of organoclay, the dispersion of individual silicate sheet is optimum. Increase in organoclay beyond a certain limit results in the formation of conglomerates, which has less cohesion with the organic phase, thus reducing mechanical properties of the hybrids. Introduction of organoclay in the hybrid materials imparts enhancement in the thermal stability and barrier properties.

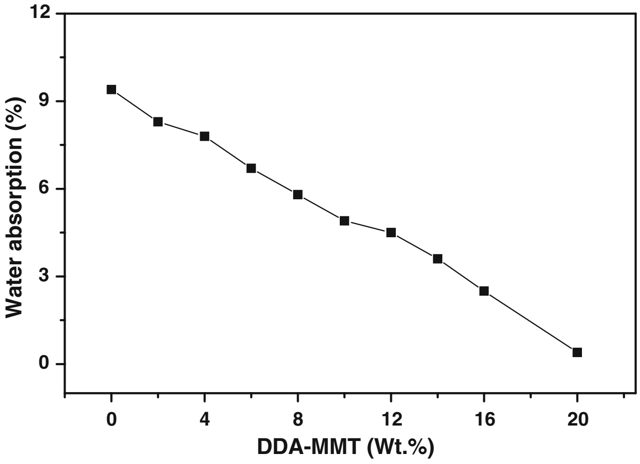

Fig. 6 Water absorption measurements of aramid/DDA-MMT nanocomposites at equilibrium

Acknowledgements The authors appreciate the financial support provided by Higher Education Commission of Pakistan (HEC) through project research grant 20-23-ACAD (R) 03-410. Sonia Zulfiqar is thankful to HEC for awarding her fellowship under “International Research Support Initiative Program” (IRSIP) to pursue research work at Max Planck Institute for Polymer Research (MPI-P), Mainz, Germany. Special thanks are due to Prof. Dr. Gerhard Wegner, Director, MPI-P for providing the characterisation facilities for the completion of this work.

References

1. Komarneni S (1992) J Mater Chem 2:1219
2. Yano Y, Usuki A, Kurauchi T, Kamigato O (1993) J Polym Sci Part A: Polym Chem 31:2493
3. Zulfiqar S, Ahmad Z, Ishaq M, Saeed S, Sarwar MI (2007) J Mater Sci 42:93
4. Giannelis EP (1996) Adv Mater 8:29
5. Vaia RA, Vasudevan S, Krawiec W, Scanlon LG, Giannelis EP (1995) Adv Mater 7:154
6. Sikka M, Cerini LN, Ghosh SS, Winey KI (1996) J Polym Sci Part B: Polym Phys 34:1443
7. Zilg C, Mulhaupt R, Finter J (1999) Macromol Chem Phys 200:661
8. Messersmith PB, Giannelis EP (1994) Chem Mater 6:1719
9. Xu R, Manias E, Snyder AJ, Runt J (2001) Macromolecules 34:337
10. Burnside SD, Giannelis EP (1995) Chem Mater 7:1597
11. Kausar A, Zulfiqar S, Shabbir S, Ishaq M, Sarwar MI (2007) Polym Bull 59:457
12. Bibi N, Sarwar MI, Ishaq M, Ahmad Z (2007) Polym Polym Compos 15:313
13. Dekany I, Szanto F, Weiss A, Lagaly G (1985) Ber Bunsenges Phys Chem 89:62
14. Dekany I, Szanto F, Nagy LG (1986) J. Colloid Interface Sci 109:376
15. Regdon I, Kiraly Z, Dekany I, Lagaly G (1994) Colloid Polym Sci 272:1129
16. Lagaly G, Dekany I (2005) Adv Colloid Interface Sci 114–115:189
17. Okada A, Kawasumi M, Usuki A, Kojimi Y, Kurauchi T, Kamigato O (1990) In: Schaefer DW, Mark JE, (eds.), Mater Res Symp Proc, Pittsburgh, vol. 171, p. 45
18. Usuki A, Kojima Y, Kawasumi M, Okada A, Fukushima Y, Kurauchi T, Kamigaito O (1993) J Mater Res 8:1179
19. Hoffmann B, Kressler J, Stopplemann G, Friedrich C, Kim G-M (2000) Colloid Polym Sci 278:629
20. Liu X, Wu Q, Zhang Q, Berglund LA, Mo Z (2002) Polym Bull 48:381
21. Hasegawa N, Okamoto H, Kato M, Usuki A, Sato N (2003) Polymer 44:2933
22. Ayyer RK, Leonov AI (2004) Rheol Acta 43:283
23. Cassidy PE (1980) Thermally Stable Polymers. Dekker, New York
24. Frazer AH (1968) High temperature resistant polymers. Wiley, New York
25. Yang HH (1993) Kevlar Aramid Fiber. Wiley, New York
26. Yang HH (1989) Aromatic high-strength fibers. Wiley, New York
27. Ahmad Z, Sarwar MI, Mark JE (1998) J Appl Polym Sci 70:297
28. Sarwar MI, Zulfiqar S, Ahmad Z (2007) Colloid Polym Sci 285:1733
29. Zulfiqar S, Ahmad Z, Sarwar MI (2007) Colloid Polym Sci 285:1749
30. Zulfiqar S, Lieberwirth I, Sarwar MI (2008) Chem Phys 344:202
31. Sarwar MI, Zulfiqar S, Ahmad Z (2008) J Sol-Gel Sci Technol 45:89
32. Zulfiqar S, Sarwar MI (2008) Scripta Mater 59:436
33. Sarwar MI, Zulfiqar S, Ahmad Z (2008) Polym Intl 57:292
34. Zulfiqar S, Ishaq M, Sarwar MI (2008) Surf Interface Anal 40:1195
35. Sarwar MI, Zulfiqar S, Ahmad Z (2007) J Sol-Gel Sci Technol 44:41
36. Zulfiqar S, Ahmad Z, Sarwar MI (2008) Polym. Adv Technol 19:1720
37. Sarwar MI, Zulfiqar S, Ahmad Z (2009) Polym Compos 30:95
38. Zulfiqar S, Lieberwirth I, Ahmad Z, Sarwar MI (2008) Polym Eng Sci 48:1624
39. Zulfiqar S, Lieberwirth I, Ahmad Z, Sarwar MI (2008) Acta Mater 56:4905
40. Wei Z, Moldowan JM, Paytan A (2006) Org Geochem 37:891
41. Zulfiqar S, Sarwar MI (2009) High Perform Polym. doi:10.1177/0954008308089114
42. Zulfiqar S, Ishaq M, Ahmad Z, Sarwar MI (2008) Polym Adv Technol 19:1250